



City Research Online

City, University of London Institutional Repository

Citation: Chen, X., Ming, Y., Fu, F. & Chen, P. (2021). Numerical and empirical modeling for the assessment of service life of RC structures in marine environment. *International Journal of Concrete Structures and Materials*,

This is the accepted version of the paper.

This version of the publication may differ from the final published version.

Permanent repository link: <https://openaccess.city.ac.uk/id/eprint/27536/>

Link to published version:

Copyright: City Research Online aims to make research outputs of City, University of London available to a wider audience. Copyright and Moral Rights remain with the author(s) and/or copyright holders. URLs from City Research Online may be freely distributed and linked to.

Reuse: Copies of full items can be used for personal research or study, educational, or not-for-profit purposes without prior permission or charge. Provided that the authors, title and full bibliographic details are credited, a hyperlink and/or URL is given for the original metadata page and the content is not changed in any way.

City Research Online:

<http://openaccess.city.ac.uk/>

publications@city.ac.uk

1
2
3
4
5
6
7
8
9
10
11
12
13
14
15
16
17
18
19
20
21
22
23
24
25
26
27
28

Numerical and empirical models for service life assessment of RC structures in marine environment

Xuandong Chen¹, Yang Ming¹, Feng Fu^{2*}, Ping Chen¹

* Corresponding author: E-mail address: feng.fu.1@city.ac.uk.

1. College of Civil Engineering and Architecture at Guilin University of Technology, China, 541004

2.School of Mathematics, Computer Science and Engineering, City, University of London, London EC1C,0HB U.K.

Received: date; Accepted: date; Published: date;

Abstract: The service life prediction of reinforced concrete (RC) structures in marine environment is essential in structural repair and health monitoring. In this paper, a numerical model for predicting the service life of reinforced concrete is first developed which considering the time-varying boundary of chloride concentration, critical chloride concentration and density of corrosion current. Based on the model, the effects of water cement ratio, reinforcement diameter, concrete cover thickness and critical chloride ion concentration on the service life and deterioration duration of RC structures are investigated. The key factors affecting the service life of reinforced concrete structures are determined. More importantly, based on regression analysis, a new simplified empirical model for predicting the service life of RC structures is also developed. It provides a fast assessment tool for practical engineers. Both the numerical model and empirical model are validated are suitable for practical engineering applications. The results show that with the increase of water cement ratio, the service life of reinforced concrete structure decreases exponentially. And with the increase of the thickness of the concrete cover, the service life, deterioration duration, and safety reserve increase linearly. However, the influence of the diameter of the reinforcing bar on the service life can be ignored..

Key words: Service life prediction; RC structures; Chloride diffusion; Critical chloride value; Corrosion current density.

1 Introduction

Reinforced concrete (RC) structures are widely used in normal construction projects , such as tall

29 buildings (Fu,2018;Fu,2021)and bridges (Fu ,2015;Fu 2016)offshore bridges, subsea tunnels, and harbour
30 projects (Pillai *et al.*, 2019; Xu, Shi ; Shao, 2019a) and . For these types of projects, chloride ingress due to
31 marine environment is one of the main factors causing the corrosion of steel bars (Marks, Glinicki and Gibas,
32 2015; Chang *et al.*, 2020). However, serious corrosion of steel bars causes the deterioration of structural
33 capacity, causing serious challenges to the durability of RC structures (Alexander and Beushausen, 2019).
34 Therefore, for marine projects, predicting the service life of the RC structure in marine environment has
35 become an important design task for design engineers. The accurate prediction enables effective health
36 monitoring and timely retrofitting of marine projects in their service life (Bouteiller, Marie-Victoire and
37 Cremona, 2016; Dhandapani *et al.*, 2018). Even for projects under construction, service life prediction can
38 provide important guidelines for designers.

39 Chloride ingress is particularly problematic to concrete (Nogueira, Leonel and Coda, 2012; Shaikh,
40 2018). Driven by the concentration difference, chloride ions and oxygen in the marine environment diffuse
41 into the interior of concrete through its pores. Unfortunately, once the chloride concentration on the steel
42 surface reaches the critical value, the passivation film on the steel surface will be destroyed. Consequently,
43 the steel reinforcement members encased are subject to corrosive damages (Guo *et al.*, 2004). This erosion
44 of the steel can cause a reduction in the RC structures' ability to resist tensile stresses. Hence, chloride ingress
45 induced reinforcement corrosion is one of the main factors affecting the durability of concrete structures and
46 at present, many scholars have carried out extensive research on this issue. Nathan D. Stambaugh *et al.*
47 (Stambaugh, Bergman and Srubar, 2018) used the critical value of chloride ion concentration on the surface
48 of steel bars as the service life assessment standard and studied the service life of RC structures in marine
49 environments under different circumstances such as the location and the mix ratio (Khanzadeh-Moradllo *et*
50 *al.*, 2015; Jung *et al.*, 2018; Mir *et al.*, 2019). However, they assumed that the chloride ion concentration on
51 the concrete surface was constant and did not consider the time-varying characteristics of the chloride ion
52 concentration on the surface (Huan, Zuquan and Xiaojie, 2015; Yang, Cai and Yu, 2017). S. Muthulingam *et*
53 *al.* (Muthulingam and Rao, 2014) established a service life prediction model by considering the influence of
54 wet-heat-diffusion coupling and the time-varying characteristics of the chloride concentration at the boundary.
55 However, the model requires too many input parameters, so it is not practical. It can only predict the moment
56 when the steel bar begins to rust, but it cannot predict when the RC structure will fail, that is, the failure life.
57 Cao *et al* (Cao, 2014) and Zhu *et al.* (Zhu and Zi, 2017; Zhang *et al.*, 2019a) established a mechanical model

58 to predict the service life of RC structures. It is based on analysis of the corrosion mechanism of steel bars
59 considering the thickness of concrete cover (Enright and Frangopol, 1998), the critical value of the chloride
60 concentration (Enright and Frangopol, 1998; Bastidas-Arteaga *et al.*, 2009), and the chloride diffusion
61 coefficient (Pack *et al.*, 2010). Zheng *et al.* (Zheng, Wong and Buenfeld, 2009) also developed a numerical
62 model to assess the influence of ITZ on the steady-state chloride diffusion. Based on the finite difference
63 method of Crank Nicolson, Song *et al.* (Song *et al.*, 2009) and Petcherdchoo *et al.* (Petcherdchoo, 2015)
64 studied the effect of retrofitting agents on the service life of RC structures. Jones *et al.* studied the
65 effectiveness of using filler to repair concrete cracks on prolonging the service life of RC structures. These
66 studies show that when micro cracks appear on the surface of concrete, repair agents can greatly prolong the
67 service life of RC structures. Furthermore, Attari *et al.* established a failure probability model for RC
68 structures. In these studies, when the failure probability reached 10%, the RC structure is considered to have
69 reached the service life, and the cracks in the RC structure have reached an acceptable limit.

70 Although many service life prediction models for RC structures have been developed, there are still
71 many challenges have not been resolved. For example, most of the existing models only use the critical
72 chloride concentration as the basis for predicting service life. However, the critical chloride concentration is
73 only the indication of beginning of steel bar corrosion (Zhao, Karimi, *et al.*, 2011). The life cycle performance
74 of reinforced concrete structures after reinforcement corrosion is rarely concerned in the existing service life
75 models. (Pan, Chen and Ruan, 2015). Most importantly, most of the existing models calculated the service
76 life of RC structures by solving complex partial differential equations, which greatly increases the
77 computational cost and is difficult to use in practical engineering. Moreover, the chloride concentration at
78 the boundary of concrete is time-dependent rather than constant, which will directly affect the distribution of
79 chloride in concrete.

80 Therefore, the focus of this research is to address above issues. The main purpose of this research is to
81 establish a practical models for practising engineers, allow them to use easily quantifying engineering
82 parameters for predicting the service life of RC structures. Firstly, a complex numerical model to predict the
83 service life of RC structures is established by diffusion-corrosion theory. The model verifications show that
84 both the chloride ion concentration and service life predictions agree well with the measured values.
85 Secondly, based on proposed model, the influence of factors such as the thickness of the cover, the water-
86 cement ratio, the critical value of chloride ion concentration, and the diameter of the reinforcement on the

87 service life of the RC structure are analysed. Finally, through a two-stage regression simulation of the service
 88 life of RC structures under 300 different conditions, an empirical model for predicting the service life of RC
 89 structures is established. By comparing with the numerical simulation results, the empirical model is in good
 90 agreement with the numerical model. The models proposed in this paper provides important theoretical
 91 support for life assessment of existing projects and optimization of service life design of projects to be built.

92 2. Theoretical background

93 2.1 Chloride diffusion model

94 After decades of theoretical and experimental research by many scholars (Hobbs, 1999; Zeng, 2007;
 95 Wang *et al.*, 2018; Zheng *et al.*, 2018; Wang, Gong and Wu, 2019), the diffusion of chloride ions in concrete
 96 in line with Fick's second law has become a widely used. And the governing equation for the diffusion of
 97 chloride ions in concrete is expressed as:

$$98 \quad \frac{dc}{dt} = \frac{\partial c}{\partial x} \left(D_c \frac{\partial c}{\partial x} \right) + \frac{\partial c}{\partial y} \left(D_c \frac{\partial c}{\partial y} \right) \quad (1)$$

99 where c is chloride ion concentration (Mass ratio of chloride ion to concrete, %), D_c is chloride ion
 100 diffusion coefficient (m^2 / s), respectively.

101 2.1.1 Chloride diffusion coefficient

102 It can be seen from Eq. (1) that the chloride ion diffusion coefficient is a key parameter that determines
 103 the diffusion rate of chloride ions in concrete. The chloride ion diffusion coefficient is not only related to the
 104 factors such as concrete types, pore structure, water-cement ratio, hydration degree, *etc.*, but also to the
 105 external environment, such as temperature (Bažant and Najjar, 1972), humidity (Muthulingam and Rao,
 106 2014), current time (Zeng, 2007). However, to simplify it, in this paper, the chloride ion diffusion coefficient
 107 is calculated with only considerations of the effects of water-cement ratio, temperature, humidity, and aging.
 108 Its expression is (Muthulingam and Rao, 2014; Chen *et al.*, 2019)

$$109 \quad D_c = \underbrace{\frac{2 \times \varphi_p^{2.75} D_p}{\varphi_p^{1.75} (3 - \varphi_p) + n(1 - \varphi_p)^{2.75}}}_{\text{Water-cement ratio}} \cdot \underbrace{\exp \left[\frac{U_c}{R} \left(\frac{1}{T_{ref}} - \frac{1}{T} \right) \right]}_{\text{Temperature}} \cdot \underbrace{\left[1 + \frac{(1-h)^4}{(1-h_c)} \right]^{-1}}_{\text{Humidity}} \cdot \underbrace{\left(\frac{t_{ref}}{t} \right)^m}_{\text{Curing age}} \quad (2)$$

110 where U_c is the activation energy for chloride ion diffusion, t_{ref} is the average exposure time, R is the
 111 gas constant, T_{ref} is the absolute ambient temperature, h is humidity, h_c is critical humidity (0.75), D_p
 112 is the diffusion coefficient of chloride ions in water, n is an empirical constant (using 14.44 as reference (Du,

113 Jin and Ma, 2014)), m is the time decay index, and f_p is the porosity of the cement slurry, respectively. f_p
 114 can be expressed as(Chen *et al.*, 2021):

$$115 \quad \varphi_p = \frac{w/c-0.17\alpha}{w/c+0.32} \quad (3)$$

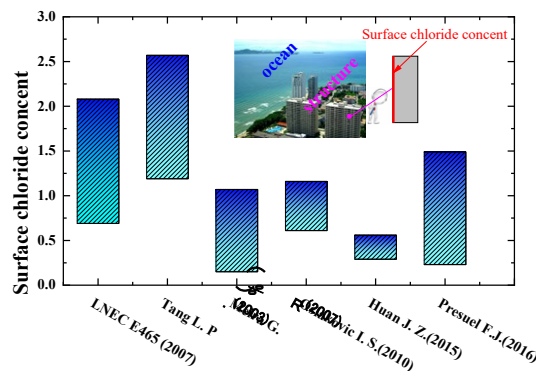
116 where α is degree of hydration of cement slurry, and w/c is water to cement ratio, respectively. The value
 117 of the degree of hydration of cement slurry α in formula (3) can be calculated by

$$118 \quad \alpha = 1 - \exp(-3.15 \times w/c) \quad (4)$$

119 2.1.2 Surface chloride ion concentration

120 The surface chloride ion concentration on the concrete is another key factor affecting the chloride ion
 121 concentration inside the concrete. In the numerical solution, the surface chloride ion concentration is also
 122 called the boundary condition. In the marine environment, chloride ions are transmitted to the surface of
 123 offshore engineering concrete structures through the flow of the air, and then diffuse into the concrete through
 124 the pores of the concrete (Yang, Cai and Yu, 2017). Fig. 1 shows statistics of chloride ion concentration on
 125 the surface of marine engineering concrete structures in different coastal areas by different scholars (Meira
 126 *et al.*, 2007; Stipanovic Oslakovic, Bjegovic and Mikulic, 2010; Huan, Zuquan and Xiaojie, 2015). It can be
 127 seen from the Fig. 1 that the surface chloride ion concentration ranges from 0.1% to 2.5%. There are many
 128 factors that affect the chloride ion concentration on the concrete surface, such as temperature, humidity,
 129 cement type, and water-binder ratio. Yang et al. and Chen et al. (YANG Lufeng, CHEN Chang, 2019)
 130 obtained the regression equation of surface chloride ion and time function through regression analysis of 372
 131 sets of surface chloride ion concentration data. It is worth noting that Eq. (5) is based on the test results of
 132 ordinary Portland concrete. Therefore, Eq. (5) is only applicable to ordinary Portland concrete, but not to
 133 special concrete, such as fly ash concrete, slag concrete, etc.

$$134 \quad C_s(t) = \frac{5.3t}{1+0.7047t} \times w/c \quad (5)$$

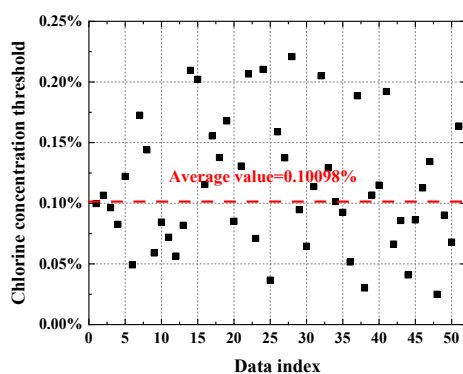


136 **Figure 1** Statistics of Surface chloride ion concentration

137 2.2 Rebar corrosion

138 2.2.1 Critical chloride ion concentration

139 Chloride ions accumulate on the surface of the steel bars over the time. When the concentration of
140 chloride ions on the surface of the steel bars reaches certain value, the steel bar begins to corrode. This value
141 is called the critical chloride ion concentration. The critical chloride ion concentration indicators include free
142 chloride ion concentration, total chloride ion concentration, and the ratio of free chloride ion concentration
143 to hydroxide concentration (Cao *et al.*, 2019). In this paper, the total chloride ion concentration is used as an
144 index to measure the critical chloride ion concentration. Due to the differences in measure methods and the
145 discrete type of concrete materials, the critical chloride ion concentration cannot be determined at present.
146 The critical chloride ion concentration currently reported is between 0.079% and 0.2% (Zhao, Hu, *et al.*,
147 2011). The critical chloride ion concentration from 51 existing literature is collected in this paper. Their
148 statistical distribution is shown in Fig. 2. From the Fig. 2, the critical chloride ion concentration distribution
149 is relatively scattered. Therefore, the mean value of 0.10098% is used in this paper as the critical chloride ion
150 concentration.



151
152 **Figure 2** Statistics of Critical chloride ion concentration

153 2.2.2 Corrosion current density

154 The chloride ion concentration is not constant across the whole volume of concrete. The chloride ion
155 concentration near the erosion surface is high, and the chloride ion concentration away from the erosion
156 surface is low (Pan, Chen and Ruan, 2015). Therefore, the chloride ion concentration on the surface near the
157 cover first reaches the critical chloride ion concentration, and the passivation film was damaged (Li, Wang
158 and Li, 2019). Research in Literature (Cao, 2014) shows that there is a potential difference between the active

159 area formed after the passivation film on the steel bar is damaged and the inert area where the passivation
 160 film is not damaged, and a macroscopic electrochemical corrosion is formed. At the same time, there is also
 161 a Micro corrosion current, the total corrosion current density can be expressed as (Zhu and Zi, 2017):

$$162 \quad i_{corr} = i_{mic} + i_{mac} \quad (6)$$

163 where i_{corr} is the total corrosion current density, i_{mic} is the micro battery corrosion current density, and i_{mac}
 164 is the macro battery corrosion current density, respectively.

165 At present, many empirical, theoretical, and numerical models have been established to calculate the
 166 corrosion current density of steel bars. In this paper, the Probabilistic mode of Papakonstantinou *et al.*
 167 (Papakonstantinou and Shinozuka, 2013) is adopted, with the expression:

$$168 \quad \ln 1.08i_{corr} = 7.89 + 0.7771 \ln(1.69c_t) - \frac{3006}{T} - 0.000116R_c \quad (7)$$

169 where i_{corr} is the corrosion current density, c_t is total chloride ion concentration, and R_c is resistance of
 170 the concrete cover, respectively.

171 The empirical formula given by Liu *et al.* (Liu and Weyers, 1998) for resistivity of concrete cover is:

$$172 \quad \ln R_c = 8.03 - 0.549 \ln(1 + 1.69c_t) \quad (8)$$

173 2.3 Determination of service life

174 In general, when the chloride ion concentration on the surface of the steel bar reaches the critical chloride
 175 ion concentration, the marine engineering concrete structure is considered to have reached the service life.
 176 The limit state function at this stage can be expressed as

$$177 \quad G_1(c, t) = C_{cri} - C(max, t) \quad (9)$$

178 where $G_1(c, t)$ is the limit state function, c_{cri} is the critical chloride ion concentration, and $c(max, t)$ is the
 179 maximum chloride ion concentration on the steel bar surface at the ingress time of t , respectively.

180 It is worth mentioning that when the maximum chloride ion concentration on the surface of the steel bar
 181 reaches the critical chloride concentration, the offshore engineering concrete structure doesn't fail, and only
 182 the steel bars begin to rust (Zhao, Hu, *et al.*, 2011; Zhao *et al.*, 2016). The radial expansion stress is developed
 183 during the corrosion process. When the radial expansion stress starts to caused damages of the the concrete
 184 cover, the cover will crack and peel, and the structure will fail (Zhao, Karimi, *et al.*, 2011). In this paper, it is
 185 called the structural failure life. The limit state function can be expressed as:

$$186 \quad G_2(lim, t) = \rho_{cr} - \rho(lim, t) \quad (10)$$

187 where ρ_{cr} is the steel rebar erosion rate at failure of the structural concrete (%), it is calculated as:

188
$$\rho_{cr} = \frac{2(\delta_1 + \delta_2)}{r_0} \quad (11)$$

189 where δ_1 is the depth of rust generated by filling the pores in the transition zone between the steel bar and
190 concrete at the interface between the corrosion products is 12.5 μm ; δ_2 is the depth of rust producing radial
191 pressure, it is worked out based on the theory of thick-walled cylinders (Xu, Shi and Shao, 2019b), and can
192 be expressed as:

193
$$\delta_2 = \frac{r_0}{E_c} \left[\frac{(r_0 + c)^2 + r_0^2}{(r_0 + c)^2 - r_0^2} + \nu_c \right] \cdot [0.3 + 0.6 c / (2r_0)] \cdot f_t \quad (12)$$

194 where r_0 is the reinforcement radius (mm), ν_c is the Poisson's ratio of the concrete cover, E_c is elastic
195 modulus of concrete (MPa), and f_t is tensile strength of concrete (MPa), respectively.

196 $\rho(\text{lim}, t)$ is the corrosion rate of steel bars at time t (%). According to Faraday's law, the distribution of
197 corrosion depth $u_d(\theta, t)$ around steel bars can be expressed as (Alexander and Beushausen, 2019; Chen *et*
198 *al.*, 2019; Zhang *et al.*, 2019):

199
$$u_d(\theta, t) = \int_{t_c}^t 0.0116 \cdot i_{corr}(\theta, t) dt \quad (13)$$

200 The mass loss of rebar can be expressed as:

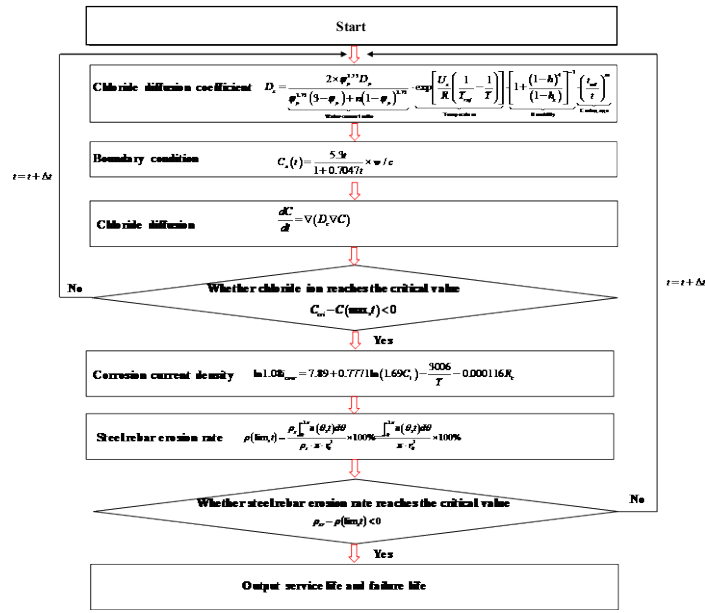
201
$$M_S = \rho_s \int_0^{2\pi} u_d(\theta, t) d\theta \quad (14)$$

202 Where ρ_s is the density of the rebar (kg/m^3):

203 So:

204
$$\rho(\text{lim}, t) = \frac{\rho_s \int_0^{2\pi} u(\theta, t) d\theta}{\rho_s \cdot \pi \cdot r_0^2} \times 100\% = \frac{\int_0^{2\pi} u(\theta, t) d\theta}{\pi \cdot r_0^2} \times 100\% \quad (15)$$

205 In the summary, the flow chart of service life prediction for RC structures is shown in Fig.3.



206

207 **Figure 3.** The Flow chart of the derivation of the proposed multiphase numeric model.

208 **3. Numerical Model validation**

209 The numerical model proposed in this paper comprises two stages modelling. The first stage is the
 210 diffusion of chloride ions, and the second stage is the corrosion of steel bars. Therefore, the model verification
 211 in this section is also divided into two aspects: chloride ion diffusion verification and service life. The
 212 parameters used in the simulation are listed in Table 1. In the process of numerical simulation, the finite
 213 difference method (FEM) is adopted to solve the chloride ion diffusion equation (Eq.1) to obtain the
 214 distribution of chloride ion concentration in concrete. Once the chloride concentration on the steel surface
 215 reaches the critical chloride concentration, the concrete structure will reach its service life. Secondly, the steel
 216 corrosion rate is calculated through the Eq (15). Once the steel corrosion rate reaches the critical steel
 217 corrosion rate, the concrete structure will reach its failure life.

218

219

220

221 **Table 1.** Numerical simulation parameters.

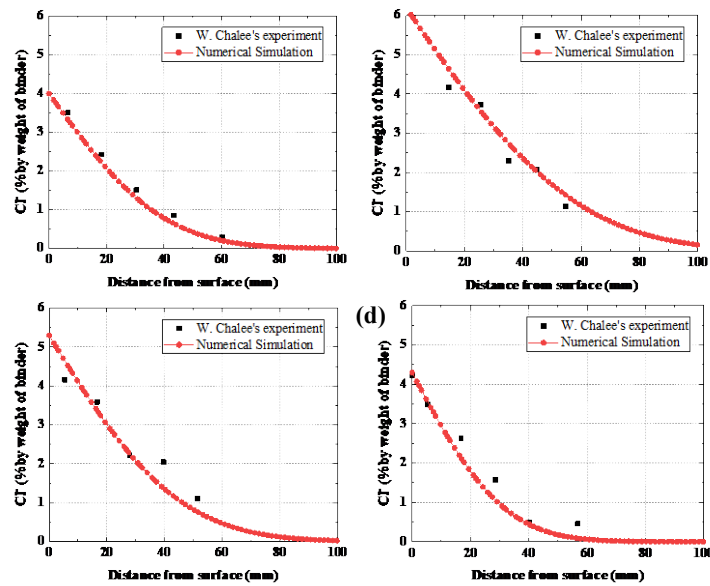
Symbol	Parameter value	Mean
U_c	44.6 [K · J/mol]	the activation energy for chloride diffusion

t_{ref}	28 [d]	Reference time of chloride ingress
R	8.314[J/K · mol]	the gas constant
h_c	0.75 [--]	the critical humidity
h	1	humidity
D_p	1.07×10^{-10} [m ² /s]	the diffusion coefficient of chloride in water
m	0.2	the time decay index of chloride diffusion
ρ_s	7500 [kg/m ³]	the density of the rebar
T_{ref}	293 [K]	reference temperature
δ_1	12.5 μ m	the depth of rust generated by filling the pores
r_0	8mm to 13mm	the reinforcement radius
E_c	30 [GPa]	elastic modulus of concrete
f_t	1.43 [MPa]	tensile strength of concrete
ν_c	0.2	the Poisson's ratio of the concrete
c	40mm to 70mm	thickness of reinforced concrete cover
w/c	0.45, 0.55, 0.65	the water to cement ratio

222 3.1 Chloride diffusion verification

223 The experimental data of W. Chalee *et al.*(Chalee, Jaturapitakkul and Chindaprasirt, 2009) will be used
224 to compare with the numerical simulation in this paper. The size of the concrete cube specimen was 200mm
225 \times 200mm \times 200 mm, and the water-cement ratio was 0.45, 0.55, 0.65. And the concrete is immersed in
226 seawater, which indicates that the concrete is saturated. Therefore, relative humidity of the concrete is 1 in
227 numerical simulation. In addition, the average value of the external ambient temperature is 293 K. The
228 comparison between numerical simulation results and test results is shown in Figure 4. Obviously, the
229 chloride concentration curve obtained by numerical simulation is very close to that obtained by experiment,

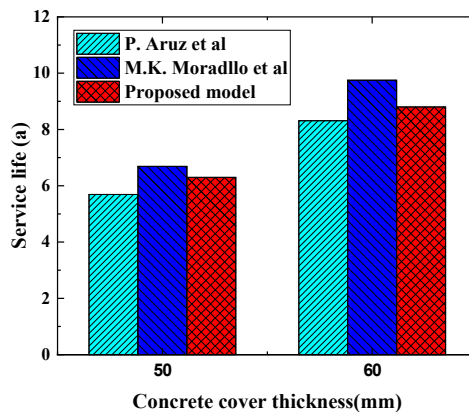
230 which indicates that the chloride diffusion model is reliable.



231
232 **Figure 4** Chloride diffusion verification (a) w/c=0.65, time=2 years; (b) w/c=0.65, time=5 years; (c) (c)
233 w/c=0.5, time=5 years;(d) w/c=0.45, time=5 years.

234 3.2 Service life verification

235 The service life prediction model proposed in this paper is compared with Moradllo *et al.* (Khazadeh
236 Moradllo, Shekarchi and Hoseini, 2012) and Aruz *et al.* (Petcherdchoo and Chindapasirt, 2019). The
237 thickness of the concrete cover is 50mm and 60mm, and the water-cement ratio is selected as 0.55. In addition,
238 the concrete is saturated, *i.e.* the relative humidity is 1. The average temperature of the environment is 293K.
239 Reinforcement diameter is 10mm. Fig. 5 shows the comparison of the service life of the three models, it can
240 be seen that the differences in the service life predictions of the three models are small, which indicates that
241 the numerical model established in this paper has a certain degree of reliability.



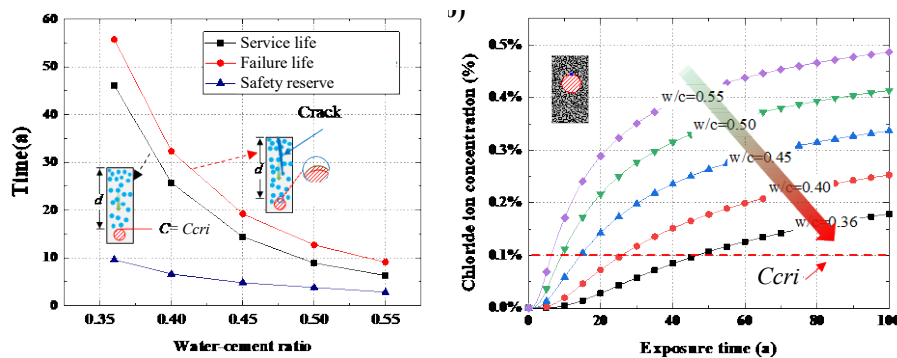
242
243 **Figure 5** Service life verification

244 **4. Parametric analysis using the new numerical model**

245 Using the proposed numerical model, intensive parametrical studies are made, which are show as
246 follows:

247 *4.1 Influence of different water-cement ratios*

248 The water-cement ratio for different concrete strength grades is different. However, different water-
249 cement ratio has great influence on the chloride diffusion coefficient and the chloride ion concentration on
250 the concrete surface, especially for the chloride diffusion coefficient(Ishida, Iqbal and Anh, 2009). Therefore,
251 the water-cement ratio has a very important influence on the durability of RC structures (Pack *et al.*, 2010).
252 Fig. 6a shows the service life of RC structures in the marine environment as a function of water-cement ratio.
253 It can be seen from the Fig. 6a that the water-cement ratio has a very important effect on the service life of
254 the marine engineering concrete structure. For example, when the water-cement ratio is 0.36, the service life
255 is 46.1 years. However, when the water-cement ratio is increased to 0.55, the service life is only 6.3 years.
256 Therefore, in marine engineering, using a low water-cement ratio can effectively increase the service life of
257 the structure. Besides, Fig. 6a also shows the relationship between the deterioration duration and the water-
258 cement ratio. The deterioration duration also decreases exponentially as the water-cement ratio increases.
259 Moreover, as the water-cement ratio increases, the safety reserve decreases more slowly. The larger the water-
260 cement ratio is, the longer the safety reserve period is, and the safety reserve period varies from 5.8 years to
261 9.8 years. Fig. 6b shows the change of the maximum chloride ion concentration on the surface of the steel
262 bar with time under different water-cement ratios. It can be seen from the Fig. 6b that under the same ingress
263 time, as the water-cement ratio increases, the chloride ion concentration gradually decreases. For example,
264 when water-cement ratio of 0.55, the maximum chloride ion concentration on the surface of the steel bar
265 increased rapidly within 0 to 20 years, and then increased slowly.

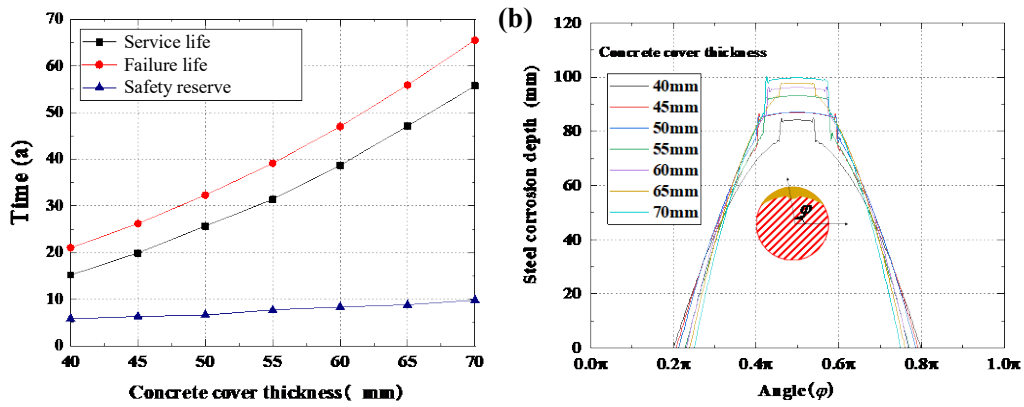


267 **Figure 6** Effect of water-cement ratio on service life and chloride concentration distribution. (a) service life;
268 (b) chloride concentration distribution

269 4.2 Thickness of concrete cover

270 The thickness of the concrete cover is an important parameter for structural design. For different
271 environments, the requirements for the thickness of the concrete cover are different in the Code for durability
272 Design of concrete structures. Therefore, it is necessary to study the effect of concrete cover thickness on
273 service life. Fig.7a shows the values of three indicators of service life, failure life, and safety reserve under
274 different concrete cover thicknesses. It can be seen from the Fig.7a that with the increase of the concrete
275 cover thickness, the service life, deterioration duration and safety reserve all increase. For example, when the
276 thickness of the cover is 40 mm, the service life is only 15.2 years. However, when the thickness of the
277 concrete cover increased to 70 mm, the service life increased to 55.7 years, which was an increase of 3.67
278 times compared to the 40 mm thickness of the concrete cover.

279 Further research found that with the increase of the thickness of the cover, the range of the change in
280 the safety reserve period was small and had a linear relationship with the thickness of the concrete cover.
281 However, deterioration duration increases greatly with the increase of the thickness of the concrete cover.
282 Fig. 7b shows the depth of the corrosion of the steel bar when the cover is cracked under different thicknesses
283 of the concrete cover. It can be seen from the Fig. 7b that the corrosion geometric form of the steel bar with
284 different cover thickness is similar, but the peak of the corrosion depth increases with the thickness of the
285 cover and increase. For instance, when the thickness of the concrete cover is 40 mm, the depth of rust is 82.3
286 μm , however, when the thickness of the concrete cover is 70 μm , the depth of rust is 100.4 μm . Moreover, the
287 corrosion depth curve of the steel bar in this paper is similar to the numerical model of Jinxia (Xia *et al.*,
288 2019), and this corrosion curve is similar to the corrosion mode of the entire steel bar observed through field
289 exposure test experiments (Sun *et al.*, 2002; Poupard *et al.*, 2006; Kessler *et al.*, 2016).



290

291 **Figure 7** Influence of concrete cover thickness on send corrosion layer depth. (a) service life (b) corrosion

292 layer depth.

293 *4.3 Influence of critical chloride ion concentration*

294 The critical chloride ion concentration is another important factor affecting the corrosion of steel bars.

295 For different types of steel bars, cement types and service environments, the critical chloride ion

296 concentration is not same. The critical chloride ion concentration obtained by many scholars has a very large

297 value (Cao, Y. *et al.* 2019, Zhang, K. *et al.* 2019). Therefore, in this section, the influence of different critical

298 chloride ion concentrations on the service life of RC structure is studied with a water-cement ratio of 0.4. As

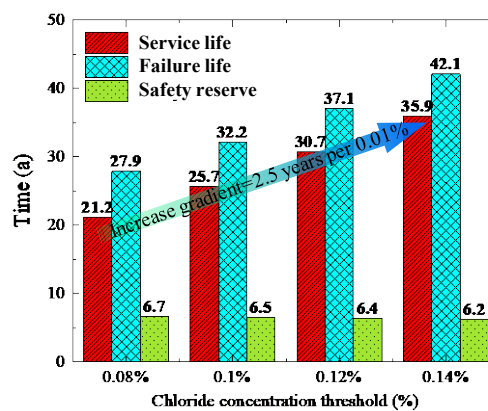
299 shown in Fig 8, as the critical chloride ion concentration increases, both the service life and the deterioration

300 duration of the RC structure increase. More importantly, it turns out that the critical chloride ion concentration

301 has a linear relationship with the service life, which is consistent with the results of S. Muthulingam *et al.*

302 (Muthulingam and Rao, 2014). For instance, for every 0.01% increase in the critical chloride ion

303 concentration, the RC structural service life increases by 2.5 years.

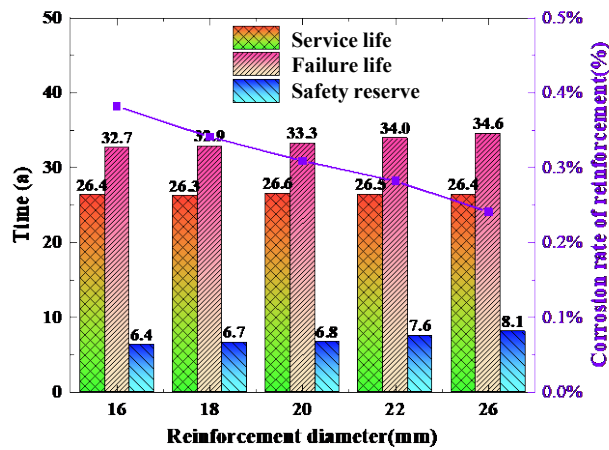


304

305 **Figure 8** Effect of critical chloride ion concentration on service life

306 4.4 Effect of Rebar Diameter

307 For different types and functions RC structures, the rebar diameter in the RC structure is also different.
308 Therefore, it is of great significance to study the impact of the rebar diameter on the service life of marine
309 RC structures. Fig. 9 shows a histogram of the service life, failure life, and safety reserve of marine RC
310 structures in the range of rebar diameters from 16 mm to 26 mm. It can be seen from the Fig. 9 that the
311 influence of the rebar diameter on the service life could be ignored (e.g., the difference between the maximum
312 and the minimum service life for different rebar diameter is only 0.5 year). This is mainly because the service
313 life mainly depends on the critical chloride concentration and thickness of concrete cover. Additionally, as
314 the diameter of the steel bar increases, the deterioration duration and safety reserve both increases, but the
315 upward trend is also slight. For example, when the rebar diameter is 16 mm, the deterioration duration and
316 safety reserve are 32.7 years and 6.4 years, respectively. And when the rebar diameter changes to 26mm, the
317 deterioration duration and safety reserve of the RC structure are 34.6 years and 8.1 years, respectively. Fig.
318 9 also shows the corrosion rate of steel bars when the structure fails under different the rebar diameters. It is
319 worth mentioning that as the rebar diameter increases, the corrosion rate of the rebar decreases significantly.
320 For example, when the rebar diameter is 16mm, the corrosion rate of the rebar is 0.382%; however, when the
321 rebar diameter is 26 mm, the rebar corrosion rate is only 0.241%.



322
323 **Figure 9** Effect of Rebar Diameter on service life

324 **5 A simplified empirical model for service life prediction**

325 According to the discussion in Section 4, it can be seen that the rebar diameter has a small effect on the
326 service life of the structure. And the thickness of the cover, the water-cement ratio and the critical chloride
327 ion concentration all have significant impact on the service life of the concrete structure. The cover thickness

328 and water-cement ratio are important parameters in engineering design. Therefore, in this paper, 300 groups
 329 RC structures with different water-cement ratios, concrete cover thickness are simulated to predict their
 330 service life. These 300 groups of data are divided into two categories. First: the thickness of the cover: 40mm,
 331 45 mm, 50 mm, 55 mm, 60 mm, 70 mm, and the water-cement ratios 0.36, 0.40, 0.50, and 0.55. Second: the
 332 cover thickness is 65 and the water-cement ratio is 0.45 as a control group. A two-stage data fitting and
 333 regression analysis method are used to establish an empirical service life prediction model. In the first stage,
 334 the functional representing the relationship between the thickness of the cover and the service life is obtained
 335 through regression analysis, as shown in formula (16), where A and B is the undetermined coefficient related
 336 to water-cement ratio. In the second stage, through regression analysis, the relationship between the
 337 undetermined coefficients A and B and the water-cement ratio is obtained, as shown in formula (17).

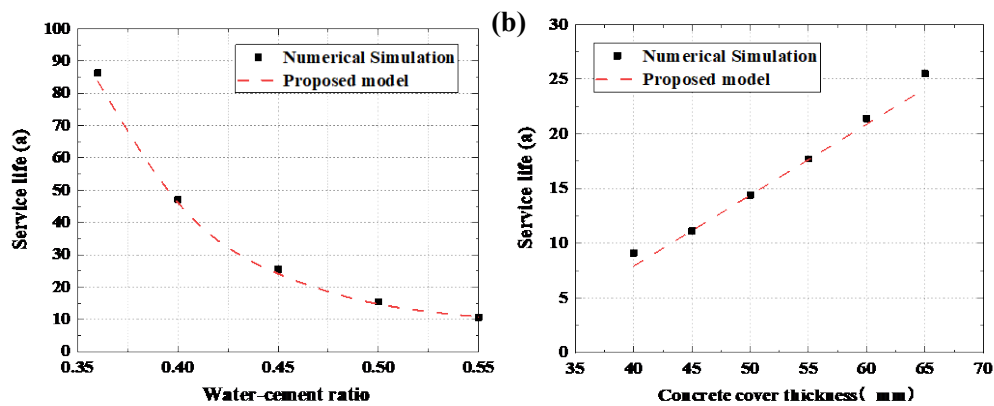
$$f(w/c, cd) = A + B \times cd \quad (16)$$

339 Where A and B is fitting parameters; w/c is water-cement ratio; cd is the thickness of concrete cover.

$$f(w/c, cd) = -4.0 + \exp\left(-\frac{326w/c}{19} + 10.364\right) + \left[\frac{2}{11} \cdot \exp\left(-\frac{137w/c}{8} + 6.945\right)\right] \times cd \quad (17)$$

341 However, in the process of numerical simulation, we assume that the ambient temperature is 293 K and the
 342 concrete is saturated. Therefore, the applicable condition of formula (17) is saturated concrete with an
 343 ambient temperature of 293 K.

344 Fig. 10 shows the comparison between the service life prediction model proposed in this paper and the
 345 numerical simulation results. It can be found that the numerical simulation results are distributed near the
 346 prediction model curve, which indicates that the proposed model in this paper is reliable.



347
 348 **Figure 10** Validation of Practical service life prediction model (a) Cover thickness=65mm; (b) Water cement
 349 ratio=0.45

350 **6 Conclusion**

351 In this paper, both numerical and empirical models for predicting the service life of RC structures in the
352 marine environment are proposed. The proposed numerical analysis model not only considers the service life
353 of RC structures, but also the deterioration duration. Moreover, the effects of water cement ratio, rebar
354 diameter, concrete cover thickness and critical chloride ion concentration on the service life and deterioration
355 duration of RC structures are comprehensively analysed, and the key factors affecting the service life of RC
356 structures are determined. The following conclusions can be drawn:

- 357 (1) With the increase of water cement ratio, the service life of RC structure decreases exponentially. When
358 the water-cement ratio is 0.36, the service life is 46.1 years. However, when the water-cement ratio is
359 increased to 0.55, the service life is only 6.3 years.
- 360 (2) With the increase of the thickness of the concrete cover, the service life, failure life, and safety reserve
361 all linear increase; Thickness of corrosion layer with different cover thickness is similar, but the peak
362 of the corrosion depth increases with the thickness of the cover increase.
- 363 (3) As the critical chloride ion concentration increases, both the service life and the deterioration duration
364 of the RC structure increase. More importantly, it turns out that the critical chloride ion concentration
365 has a linear relationship with the service life.
- 366 (4) The influence of the rebar diameter on the service life can be ignored. It is worth mentioning that as the
367 rebar diameter increases, the corrosion rate of steel bars decreases significantly.
- 368 (5) Various factors (water-cement ratio, protective layer thickness, rebar diameter, *etc.*) have a small impact
369 on the safety reserve period. The safety reserve period of RC structure is generally less than 10 years.
- 370 (6) Through regression analysis of 300 sets of simulation data, the proposed empirical forecasting model has
371 good reliability in the service life prediction of RC structures and is suitable for practical engineers.

372 **Availability of data and materials**

373 All data that support the findings of this study are available from the corresponding author upon reasonable
374 request.

375 **Competing interests**

376 The authors declare no conflict of interest.

377 **Funding**

378 National Natural Science Foundation of China (No. 51968014,51968013),

379 Guangxi Key Laboratory of New Energy and Building Energy Saving Foundation (No. 19-J-21-4, 19-J-21-
380 30),

381 Guangxi Universities Scientific Research Project (2020KY06029).

382 **Author Contributions:**

383 **Xuandong Chen:** Writing- Original draft preparation, Data curation, Writing, Conceptualization,
384 Methodology, Investigation. **Feng Fu:** Writing- Original draft preparation, Writing- Reviewing and Editing,
385 Methodology, Investigation. **Ping Chen:** Validation, Software. **Yang Ming:** Software, Data curation.

386 **Acknowledgements:**

387 Authors appreciate the financial supports from the National Natural Science Foundation of China (No.
388 51968014,51968013), Guangxi Key Laboratory of New Energy and Building Energy Saving Foundation (No.
389 19-J-21-4, 19-J-21-30), and Guangxi Universities Scientific Research Project (2020KY06029).

390 **Authors' information**

391 **Xuandong Chen** MSc, lecturer, College of Civil Engineering and Architecture, Guilin University of
392 Technology, Guilin 541004, China; China. Guangxi Key Laboratory of New Energy and Building Energy
393 Saving, Guilin 541004, China; Guangxi Engineering and Technology Center for Utilization of Industrial
394 Waste Residue in Building Materials, Guilin, 541004, China. E-mail: 6616051@glut.edu.cn

395

396 **Yang Ming**, MSc, Engineer, Guangxi Engineering and Technology Center for Utilization of Industrial Waste
397 Residue in Building Materials, Guilin, 541004, China. 574081667@qq.com

398

399 **Feng Fu**, PhD Associate Professor, School of Mathematics, Computer Science and Engineering, City,
400 University of London, London EC1C,0HB U.K. (corresponding author) feng.fu.1@city.ac.uk; Professor,
401 College of Civil Engineering and Architecture, Guilin University of Technology, Guilin 541004, China

402 **Ping Chen** PhD, Senior Research Fellow, Guangxi Engineering and Technology Center for Utilization of

403 Industrial Waste Residue in Building Materials, Guilin, 541004, China., chenping8383@188.com

404

405 **Xiang Hu** MSc, lecturer, College of Civil Engineering and Architecture, Guilin University of Technology,
406 Guilin 541004, China; China. Guangxi Key Laboratory of New Energy and Building Energy Saving, Guilin
407 541004, China. E-mail: 6616050@glut.edu.cn

408

409 **Reference**

410 Alexander, M. and Beushausen, H. (2019) 'Durability, service life prediction, and modelling for reinforced
411 concrete structures – review and critique', *Cement and Concrete Research*, 122(May), pp. 17–29. doi:
412 10.1016/j.cemconres.2019.04.018.

413 Bastidas-Arteaga, E. *et al.* (2009) 'Probabilistic lifetime assessment of RC structures under coupled corrosion-
414 fatigue deterioration processes', *Structural Safety*, 31(1), pp. 84–96. doi: 10.1016/j.strusafe.2008.04.001.

415 Bažant, Z. P. and Najjar, L. J. (1972) 'Nonlinear water diffusion in nonsaturated concrete', *Matériaux et*
416 *Constructions*, 5(1), pp. 3–20. doi: 10.1007/BF02479073.

417 Bouteiller, V., Marie-Victoire, E. and Cremona, C. (2016) 'Mathematical relation of steel thickness loss with
418 time related to reinforced concrete contaminated by chlorides', *Construction and Building Materials*, 124, pp.
419 764–775. doi: 10.1016/j.conbuildmat.2016.07.078.

420 Cao, C. (2014) '3D simulation of localized steel corrosion in chloride contaminated reinforced concrete',
421 *Construction and Building Materials*, 72, pp. 434–443. doi: 10.1016/j.conbuildmat.2014.09.030.

422 Cao, Y. *et al.* (2019) 'Critical chloride content in reinforced concrete — An updated review considering Chinese
423 experience', *Cement and Concrete Research*, 117(November 2018), pp. 58–68. doi:
424 10.1016/j.cemconres.2018.11.020.

425 Chalee, W., Jaturapitakkul, C. and Chindaprasirt, P. (2009) 'Predicting the chloride penetration of fly ash
426 concrete in seawater', *Marine Structures*, 22(3), pp. 341–353. doi: 10.1016/j.marstruc.2008.12.001.

427 Chang *et al.* (2020) 'Durability and Aesthetics of Architectural Concrete under Chloride Attack or Carbonation',
428 *Materials*, 13(4), p. 839. doi: 10.3390/ma13040839.

429 Chen, X. *et al.* (2019) 'Meso-numerical Simulation of Service Life Prediction for Marine Structures', *Journal of*

430 *Building Materials*, 22(6), pp. 894–900. doi: 10.3969/j.issn.1007-9629.2019.06.009.

431 Chen, X. *et al.* (2021) ‘A multi-phase mesoscopic simulation model for the long-term chloride ingress and
432 electrochemical chloride extraction’, *Construction and Building Materials*, 270, p. 121826. doi:
433 10.1016/j.conbuildmat.2020.121826.

434 Dhandapani, Y. *et al.* (2018) ‘Mechanical properties and durability performance of concretes with Limestone
435 Calcined Clay Cement (LC3)’, *Cement and Concrete Research*, 107(March), pp. 136–151. doi:
436 10.1016/j.cemconres.2018.02.005.

437 Du, X., Jin, L. and Ma, G. (2014) ‘A meso-scale numerical method for the simulation of chloride diffusivity in
438 concrete’, *Finite Elements in Analysis and Design*, 85, pp. 87–100. doi: 10.1016/j.finel.2014.03.002.

439 Enright, M. P. and Frangopol, D. M. (1998) ‘Probabilistic analysis of resistance degradation of reinforced
440 concrete bridge beams under corrosion’, *Engineering Structures*, 20(11), pp. 960–971. doi: 10.1016/S0141-
441 0296(97)00190-9.

442 Fu, F. (2018). *Design and Analysis of Tall and Complex Structures*. Butterworth-Heinemann. ISBN 978-0-08-
443 101121-8.

444 Fu, F. (2015). *Advanced Modeling Techniques in Structural Design*. John Wiley & Sons. ISBN 978-1-118-
445 82543-3

446 Fu, F. (2016). *Structural Analysis and Design to Prevent Disproportionate Collapse*. CRC Press. ISBN 978-1-
447 4987-0680-3.

448 Fu, F. (2018). *Design and Analysis of Tall and Complex Structures*. Butterworth-Heinemann. ISBN 978-0-08-
449 101121-8.

450 Fu, F. (2021). *Fire Safety Design for Tall Buildings*. Taylor Francis. ISBN 978-0-367-44452-5.

451 Guo, H. *et al.* (2004) ‘Durability of recycled aggregate concrete - A review’, *Cement and Concrete Composites*,
452 26(2), pp. 97–98. doi: 10.1016/S0958-9465(03)00091-X.

453 Hobbs, D. W. (1999) ‘Aggregate influence on chloride ion diffusion into concrete’, *Cement and Concrete*
454 *Research*, 29(12), pp. 1995–1998. doi: 10.1016/S0008-8846(99)00188-X.

455 Huan, X. U. E., Zuquan, J. I. N. and Xiaojie, W. (2015) ‘Chloride ion penetration into concrete exposed to

456 marine environment for a long period', *THE OCEAN ENGINEER RING*, 33(5), pp. 60–65. doi: 10. 16483 /
457 j. issn. 1005-9865. 2015. 05. 008.

458 Ishida, T., Iqbal, P. O. N. and Anh, H. T. L. (2009) 'Modeling of chloride diffusivity coupled with non-linear
459 binding capacity in sound and cracked concrete', *Cement and Concrete Research*, 39(10), pp. 913–923. doi:
460 10.1016/j.cemconres.2009.07.014.

461 Jung, S.-H. *et al.* (2018) 'Maintenance for Repaired RC Column Exposed to Chloride Attack Based on
462 Probability Distribution of Service Life', *International Journal of Concrete Structures and Materials*, 12(1), p.
463 22. doi: 10.1186/s40069-018-0259-2.

464 Kessler, S. *et al.* (2016) 'Effect of freeze–thaw damage on chloride ingress into concrete', *Materials and*
465 *Structures*, 50(2), p. 121. doi: 10.1617/s11527-016-0984-4.

466 Khanzadeh-Moradllo, M. *et al.* (2015) 'Effect of Wet Curing Duration on Long-Term Performance of Concrete
467 in Tidal Zone of Marine Environment', *International Journal of Concrete Structures and Materials*, 9(4), pp.
468 487–498. doi: 10.1007/s40069-015-0118-3.

469 Khanzadeh Moradllo, M., Shekarchi, M. and Hoseini, M. (2012) 'Time-dependent performance of concrete
470 surface coatings in tidal zone of marine environment', *Construction and Building Materials*, 30, pp. 198–205.
471 doi: 10.1016/j.conbuildmat.2011.11.044.

472 Li, D., Wang, X. and Li, L. yuan (2019) 'An analytical solution for chloride diffusion in concrete with
473 considering binding effect', *Ocean Engineering*, 191(October), p. 106549. doi:
474 10.1016/j.oceaneng.2019.106549.

475 Liu, Y. and Weyers, R. E. (1998) 'Modeling the Time-to-Corrosion Cracking in Chloride Contaminated
476 Reinforced Concrete Structures', *ACI Materials Journal*, 95(6). doi: 10.14359/410.

477 Marks, M., Glinicki, M. A. and Gibas, K. (2015) 'Prediction of the chloride resistance of concrete modified with
478 high calcium fly ash using machine learning', *Materials*, 8(12), pp. 8714–8727. doi: 10.3390/ma8125483.

479 Meira, G. R. *et al.* (2007) 'Chloride penetration into concrete structures in the marine atmosphere zone -
480 Relationship between deposition of chlorides on the wet candle and chlorides accumulated into concrete',
481 *Cement and Concrete Composites*, 29(9), pp. 667–676. doi: 10.1016/j.cemconcomp.2007.05.009.

482 Mir, Z. M. *et al.* (2019) 'Enhanced Predictive Modelling of Steel Corrosion in Concrete in Submerged Zone

483 Based on a Dynamic Activation Approach', *International Journal of Concrete Structures and Materials*, 13(1),
484 p. 11. doi: 10.1186/s40069-018-0321-0.

485 Muthulingam, S. and Rao, B. N. (2014) 'Non-uniform time-to-corrosion initiation in steel reinforced concrete
486 under chloride environment', *Corrosion Science*, 82, pp. 304–315. doi: 10.1016/j.corsci.2014.01.023.

487 Nogueira, C., Leonel, E. and Coda, H. (2012) 'Probabilistic failure modelling of reinforced concrete structures
488 subjected to chloride penetration', *International Journal of Advanced Structural Engineering*, 4(1), p. 10. doi:
489 10.1186/2008-6695-4-10.

490 Pack, S. W. *et al.* (2010) 'Prediction of time dependent chloride transport in concrete structures exposed to a
491 marine environment', *Cement and Concrete Research*, 40(2), pp. 302–312. doi:
492 10.1016/j.cemconres.2009.09.023.

493 Pan, Z., Chen, A. and Ruan, X. (2015) 'Spatial variability of chloride and its influence on thickness of concrete
494 cover: A two-dimensional mesoscopic numerical research', *Engineering Structures*, 95, pp. 154–169. doi:
495 10.1016/j.engstruct.2015.03.061.

496 Papakonstantinou, K. G. and Shinozuka, M. (2013) 'Probabilistic model for steel corrosion in reinforced
497 concrete structures of large dimensions considering crack effects', *Engineering Structures*, 57, pp. 306–326. doi:
498 10.1016/j.engstruct.2013.06.038.

499 Petcherdchoo, A. (2015) 'Repairs by fly ash concrete to extend service life of chloride-exposed concrete
500 structures considering environmental impacts', *Construction and Building Materials*, 98, pp. 799–809. doi:
501 10.1016/j.conbuildmat.2015.08.120.

502 Petcherdchoo, A. and Chindapasirt, P. (2019) 'Exponentially aging functions coupled with time-dependent
503 chloride transport model for predicting service life of surface-treated concrete in tidal zone', *Cement and*
504 *Concrete Research*, 120(October 2017), pp. 1–12. doi: 10.1016/j.cemconres.2019.03.009.

505 Pillai, R. G. *et al.* (2019) 'Service life and life cycle assessment of reinforced concrete systems with limestone
506 calcined clay cement (LC3)', *Cement and Concrete Research*, 118(July 2018), pp. 111–119. doi:
507 10.1016/j.cemconres.2018.11.019.

508 Poupard, O. *et al.* (2006) 'Corrosion damage diagnosis of a reinforced concrete beam after 40 years natural
509 exposure in marine environment', *Cement and Concrete Research*, 36(3), pp. 504–520. doi:

510 10.1016/j.cemconres.2005.11.004.

511 Shaikh, F. U. A. (2018) 'Effect of Cracking on Corrosion of Steel in Concrete', *International Journal of*
512 *Concrete Structures and Materials*, 12(1), p. 3. doi: 10.1186/s40069-018-0234-y.

513 Song, H. W. *et al.* (2009) 'Service life prediction of repaired concrete structures under chloride environment
514 using finite difference method', *Cement and Concrete Composites*, 31(2), pp. 120–127. doi:
515 10.1016/j.cemconcomp.2008.11.002.

516 Stambaugh, N. D., Bergman, T. L. and Srubar, W. V. (2018) 'Numerical service-life modeling of chloride-
517 induced corrosion in recycled-aggregate concrete', *Construction and Building Materials*, 161, pp. 236–245. doi:
518 10.1016/j.conbuildmat.2017.11.084.

519 Stipanovic Oslakovic, I., Bjegovic, D. and Mikulic, D. (2010) 'Evaluation of service life design models on
520 concrete structures exposed to marine environment', *Materials and Structures/Materiaux et Constructions*,
521 43(10), pp. 1397–1412. doi: 10.1617/s11527-010-9590-z.

522 Sun, W. *et al.* (2002) 'Effect of chloride salt, freeze–thaw cycling and externally applied load on the
523 performance of the concrete', *Cement and Concrete Research*, 32(12), pp. 1859–1864. doi: 10.1016/S0008-
524 8846(02)00769-X.

525 Wang, Y., Gong, X. and Wu, L. (2019) 'Prediction model of chloride diffusion in concrete considering the
526 coupling effects of coarse aggregate and steel reinforcement exposed to marine tidal environment', *Construction*
527 *and Building Materials*, 216, pp. 40–57. doi: 10.1016/j.conbuildmat.2019.04.221.

528 Wang, Yuanzhan *et al.* (2018) 'Prediction model of long-term chloride diffusion into plain concrete considering
529 the effect of the heterogeneity of materials exposed to marine tidal zone', *Construction and Building Materials*,
530 159, pp. 297–315. doi: 10.1016/j.conbuildmat.2017.10.083.

531 Xia, J. *et al.* (2019) 'Numerical simulation of steel corrosion in chloride contaminated concrete', *Construction*
532 *and Building Materials*, 228, p. 116745. doi: 10.1016/j.conbuildmat.2019.116745.

533 Xu, Q., Shi, D. and Shao, W. (2019a) 'Service life prediction of RC square piles based on time-varying
534 probability analysis', *Construction and Building Materials*, 227, p. 116824. doi:
535 10.1016/j.conbuildmat.2019.116824.

536 Xu, Q., Shi, D. and Shao, W. (2019b) 'Service life prediction of RC square piles based on time-varying

537 probability analysis', *Construction and Building Materials*, 227, p. 116824. doi:
538 10.1016/j.conbuildmat.2019.116824.

539 Yang, L., Cai, R. and Yu, B. (2017) 'Formation mechanism and multi-factor model for surface chloride
540 concentration of concrete in marine atmosphere zone', *Tumu Gongcheng Xuebao/China Civil Engineering*
541 *Journal*, 50(12), pp. 46–55. doi: 10.15951/j.tmgcxb.2017.12.006.

542 YANG Lufeng, CHEN Chang, Y. B. (2019) 'Multi-factor Time-varying Model of Marine Environmental Action
543 on Concrete in Splash Zone', *JOURNAL OF THE CHINESE CERAMIC SOCIETY*, 11(47), pp. 1566–1572.

544 Zeng, Y. (2007) 'Modeling of chloride diffusion in hetero-structured concretes by finite element method',
545 *Cement and Concrete Composites*, 29(7), pp. 559–565. doi: 10.1016/j.cemconcomp.2007.04.003.

546 Zhang, K. *et al.* (2019) 'Analytical model for critical corrosion level of reinforcements to cause the cracking of
547 concrete cover', *Construction and Building Materials*, 223, pp. 185–197. doi:
548 10.1016/j.conbuildmat.2019.06.210.

549 Zhao, Y., Karimi, A. R., *et al.* (2011) 'Comparison of uniform and non-uniform corrosion induced damage in
550 reinforced concrete based on a Gaussian description of the corrosion layer', *Corrosion Science*, 53(9), pp. 2803–
551 2814. doi: 10.1016/j.corsci.2011.05.017.

552 Zhao, Y., Hu, B., *et al.* (2011) 'Non-uniform distribution of rust layer around steel bar in concrete', *Corrosion*
553 *Science*, 53(12), pp. 4300–4308. doi: 10.1016/j.corsci.2011.08.045.

554 Zhao, Y. *et al.* (2016) 'Non-uniform distribution of a corrosion layer at a steel/concrete interface described by a
555 Gaussian model', *Corrosion Science*, 112, pp. 1–12. doi: 10.1016/j.corsci.2016.06.021.

556 Zheng, J. J. *et al.* (2018) 'A numerical algorithm for evaluating the chloride diffusion coefficient of concrete
557 with crushed aggregates', *Construction and Building Materials*, 171, pp. 977–983. doi:
558 10.1016/j.conbuildmat.2018.03.184.

559 Zheng, J. jun, Wong, H. S. and Buenfeld, N. R. (2009) 'Assessing the influence of ITZ on the steady-state
560 chloride diffusivity of concrete using a numerical model', *Cement and Concrete Research*, 39(9), pp. 805–813.
561 doi: 10.1016/j.cemconres.2009.06.002.

562 Zhu, X. and Zi, G. (2017) 'A 2D mechano-chemical model for the simulation of reinforcement corrosion and
563 concrete damage', *Construction and Building Materials*, 137, pp. 330–344. doi:

564 10.1016/j.conbuildmat.2017.01.103.

565

566

567